

# Lanthanide Features in Near-infrared Spectra of Kilonovae

[Nanae Domoto](#), [Masaomi Tanaka](#), [Daiji Kato](#), [Kyohei Kawaguchi](#), [Kenta Hotokezaka](#), [Shinya Wanajo](#)

## ABSTRACT

The observations of GW170817/AT2017gfo have provided us with evidence that binary neutron star mergers are sites of *r*-process nucleosynthesis. However, the observed signatures in the spectra of GW170817/AT2017gfo have not been fully decoded especially in the near-infrared (NIR) wavelengths. In this paper, we investigate the kilonova spectra over the entire wavelength range with the aim of elemental identification. We systematically calculate the strength of bound-bound transitions by constructing a hybrid line list that is accurate for important strong transitions and complete for weak transitions. We find that the elements on the left side of the periodic table, such as Ca, Sr, Y, Zr, Ba, La, and Ce, tend to produce prominent absorption lines in the spectra. This is because such elements have a small number of valence electrons and low-lying energy levels, resulting in strong transitions. By performing self-consistent radiative transfer simulations for the entire ejecta, we find that La III and Ce III appear in the NIR spectra, which can explain the absorption features at  $\lambda \sim 12000\text{--}14000\text{ \AA}$  in the spectra of GW170817/AT2017gfo. The mass fractions of La and Ce are estimated to be  $> 2 \times 10^{-6}$  and  $\sim (1\text{--}100) \times 10^{-5}$ , respectively. An actinide element Th can also be a source of absorption as the atomic structure is analogous to that of Ce. However, we show that Th III features are less prominent in the spectra because of the denser energy levels of actinides compared to those of lanthanides.

## 中性子星合体

r-process元素を合成、それらが放射性崩壊を起こすことで可視光・赤外線域での放射、**キロノバ**を生じると期待

→ **GW170817**の観測によって、連星中性子星合体がr-process元素合成の場である証拠を得た

• GW170817の観測→ストロンチウムのみ確認されている(Watson et al. 2019) (8000 Å 付近の吸収)

• キロノバのスペクトルから合成された元素を同定するには、分光学的に正確な原子のデータが必要

→ NIRの重元素については原子データが完全ではない

→ 理論計算だけでなく実験データとの較正が必要

• NIR域のキロノバスペクトルはまだ十分に調べられていない

→ 全波長域に渡るキロノバスペクトルを調査

• 元素を同定するため、NS合体ejectaにおける束縛-束縛遷移の線強度の計算と、放射伝達シミュレーションを行った

## Line list

遷移の波長、遷移のエネルギー準位、遷移確率のデータセット

\* 線強度を評価するには原子データが必要

## Hybrid line list

・ 理論計算→完全なラインリスト

NS合体ejectaの物理的条件下で、どの元素が強い遷移を示すか同定

・ 理論的なエネルギー準位を実験データで較正

→ 強い遷移を示すイオンの正確なラインリストを構築

⇒ 元素同定に重要な、強い遷移(line)は正確、弱い遷移は完全な

**Hybrid line list**

- ・ キロノバスペクトルにおいて吸収源となる元素を調べるため、与えられた密度・温度・元素量に対して束縛-束縛遷移の線強度を系統的に計算
- ・ 線強度は**Sobolev optical depth** (Sobolev 1960)で近似

$$\begin{aligned}\tau_l &= \frac{\pi e^2}{m_e c} n_{i,j,k} t \lambda_l f_l \\ &= \frac{\pi e^2}{m_e c} n_{i,j} t \lambda_l f_l \frac{g_k}{g_0} e^{-\frac{E_k}{kT}},\end{aligned}$$

$n_{i,j,k}$ : 遷移のlower levelのイオン数密度

$\lambda_l, f_l$ : 遷移波長、振動子強度

$g_0$ : 基底状態での統計的重み

$g_k, E_k$ : 束縛-束縛遷移の統計的重みlower

エネルギー準位

LTEを仮定

NS合体によるejectaの存在量

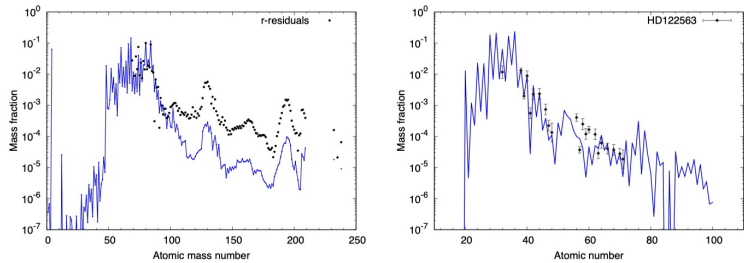


**Figure 1.** Left: final abundances of our L model as a function of mass number. Black circles show the *r*-process residual pattern (Prantzos et al. 2020), which are scaled to match those for the L model at  $A = 88$ . Right: abundances at  $t = 1.5$  days as a function of atomic number. Abundances of an *r*-process-deficient star HD 122563 (diamonds, Honda et al. 2006; Ge from Cowan et al. 2005; Cd and Lu from Roederer et al. 2012) are also shown for comparison, which are scaled to match those for the L model at  $Z = 40$ .

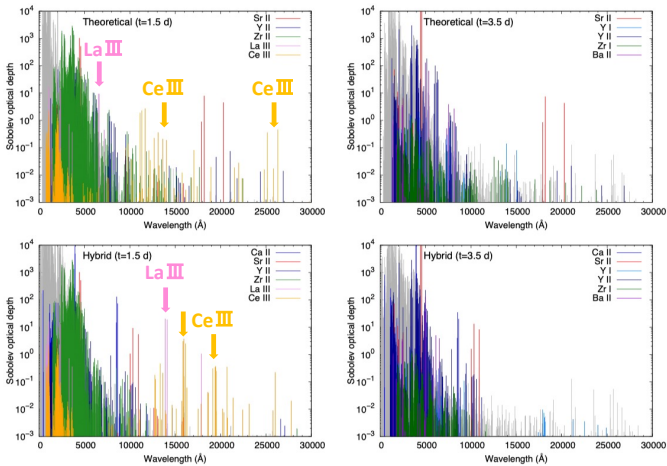


**Figure 2.** Sobolev optical depth of bound-bound transitions for the L model calculated with the theoretical line list (Tanaka et al. 2020,  $Z = 30\text{--}88$ , top) and those calculated with the hybrid line list ( $Z = 20\text{--}88$ , bottom, Section 2.3). The ions with large contributions are shown with colors. The left panels show the results with the density of  $\rho = 10^{-14}\text{ g cm}^{-3}$  and the temperature of  $T = 5000\text{ K}$  at  $t = 1.5$  days, while the right panels show those with  $\rho = 10^{-15}\text{ g cm}^{-3}$  and  $T = 3000\text{ K}$  at  $t = 3.5$  days.

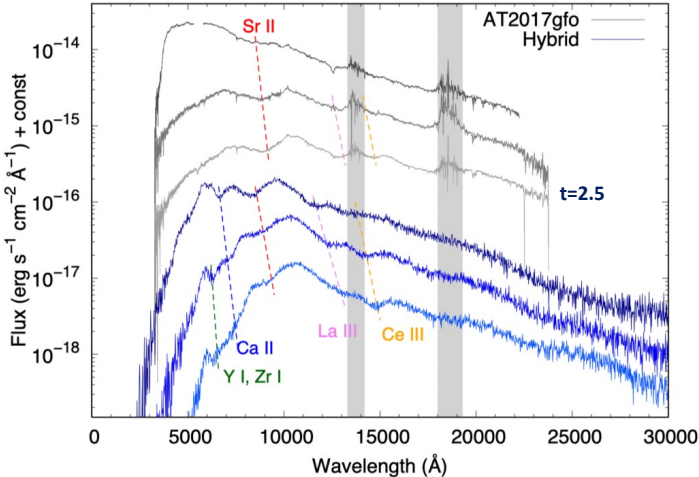


**Figure 8.** Comparison between the synthetic spectra (blue) and the observed spectra of AT2017gfo (gray, Pian et al. 2017; Smartt et al. 2017) at  $t = 1.5, 2.5$ , and  $3.5$  days after the merger (dark to light colors). Spectra are vertically shifted for visualization. Gray shade shows the regions of strong atmospheric absorption.

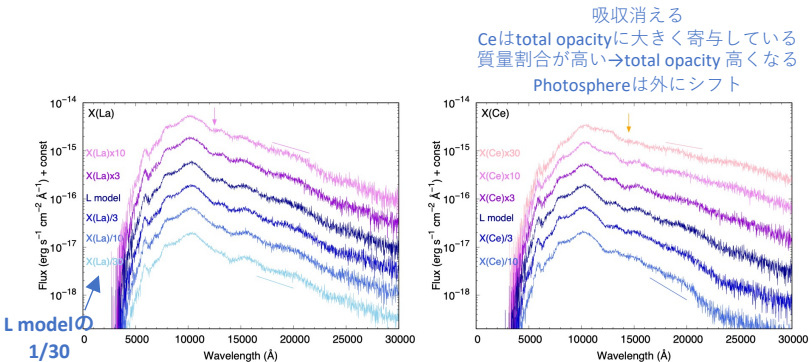


**Figure 9.** Synthetic spectra at  $t = 2.5$  days after the merger for different mass fractions of La (left) and Ce (right). Variation of each element is shown in the legend with the same color used for the spectra. Pink and orange arrows in each panel indicate the position of the notable absorption lines caused by La III and Ce III, respectively. Line segments above and below the spectra indicate spectral slopes for visualization.

・ La IIIとCe IIIが近赤外線波長域 ( $\lambda \sim 12000\text{--}14000\text{ \AA}$ ) で吸収特性を持つことを発見

→ GW170817のスペクトルと一致

・ La IIIとCe IIIによる吸収線を用いて、GW170817/AT2017gfoのejectaで合成されたLaとCeのmas fraction (ある部分での質量の割合)を求めた

・  $X(La) > 2 \times 10^{-6}$

・  $X(Ce) \sim (1 - 100) \times 10^{-5}$

→ NS合体ejectaのランタノイド存在比を分光学的に推定した、初めての例

・ アクチノイド元素の同定には別の方法が必要

・ この論文では軽いr-process元素に支配されたモデルを使用

→ ランタノイドが豊富なejectaは議論できない

ランタノイドが豊富なejectaは重元素のopacityが高い

→ スペクトルはより暗く、赤くなる

→ 重元素からの弱い線が多く存在するのでスペクトルはより滑らかになる